High-Speed and High-Power Vertical-Cavity Surface-Emitting Lasers based on InP suitable for Telecommunication and Gas Sensing

Tobias Gruendl*[a], Karolina Zogal[c], Michael Mueller[a], Robin D. Nagel[a], Sandro Jatta[c], Kathrin Geiger[a], Christian Grasse[a], Gerhard Boehm[a], Markus Ortsiefer[b], Ralf Meyer[a], Peter Meissner[c], Markus-Christian Amann[a]

[a]Walter Schottky Institut, Technische Universitaet Muenchen, Lehrstuhl für Halbleitertechnologie, Am Coulombwall 3, 85748 Garching, Germany

[b]VERTILAS GmbH, Lichtenbergstrasse 8, 85748 Garching, Germany

[c]Technische Universitaet Darmstadt, Institut für Optische Nachrichtentechnik, Merckstrasse 25, 64283 Darmstadt, Germany

*Gruendl@wsi.tum.de; phone +49-89-289-12789; fax +49-89-289-12737; www.wsi.tum.de

ABSTRACT

We present 1.55 µm short-cavity buried-tunnel-junction VCSELs (Vertical-Cavity Surface-Emitting Lasers) with single mode output powers of 6.7 mW at 20°C and 3 mW at 80°C, respectively. Although the device had been predominantly optimized for high-power applications and a proper heat management, we are also observing a 3dB-cut-off frequency of more than 11 GHz and side mode suppression ratios (SMSRs) beyond 54 dB over the whole temperature range. The tuning range of the devices can be increased from 7 nm based on gain tuning to several tens of nanometers when replacing the top DBR by a micro-electro-mechanical system (MEMS) distributed Bragg reflector (DBR) composed of semiconductor or dielectric material being thermally actuated for changing the cavity length. These devices are perfectly suitable for telecommunication and gas sensing applications and represent outstanding devices for the so called tunable diode laser absorption spectroscopy (TDLAS) technique.

Keywords: MEMS VCSEL, InP, High-Speed, High-Power, Wide Tunability, Telecommunication, Gas Sensing

1. INTRODUCTION

In our nowadays very globalized high-tech world, there are two very important application fields which have been arisen over the past few years. On the one hand, the fiber based telecommunication sector offering a new dimension of exchanging big amount of data worldwide and on the other hand a more environmentally driven aspect, that is the demand for gas sensing and spectroscopy. While the first sector is representing the basis for ultra-high-definition TV and video, USB 3.0, video conferences and telephone calls held via internet, the second one is offering direct access to check and optimize for instance the efficiency of vehicles' engines, to investigate the air pollution, and to detect the amount of CO, CO_2, NH_3, C_2H_2 in exhausted fumes [1]. Each one of these mentioned gases show sufficiently strong absorption lines within the 1.52-1.58 µm wavelength range and could be easily detectable by a tunable laser device with a tuning range exceeding 60 nm. In many cases these tunable devices can be perceived as sensors which are serving as interlock and security systems. Taking into account the discussion about oil platforms in this year one can imagine how beneficially the application of these kind of sensors could be.

At first glance these topics (telecommunication and sensing) don't have anything in common with each other. However, both of them have become more and more interesting within the past decade as in particular semiconductor devices have been developed and of course successively optimized. While predominantly LEDs are nowadays used for the general

lightening of buildings and houses (both for public and private usage) and even in cars (LED headlamp substituting the former light bulb), lasers and semiconductor based detectors gained increasing interest for telecommunication via fiber optics, for entertainment (i.e. laser shows), military use (night vision device), static observations of buildings via fibre-bragg-gratings [1] and of course spectroscopy and gas sensing. For instance the detection of methane (CH_4) and Ammonia (NH_3) has already been successfully demonstrated in former time [2,3]. The key-element among all existing semiconductor laser devices fitting best to these requirements is undoubtedly the Vertical-Cavity Surface-Emitting Laser (abbreviation: VCSEL) which has been firstly presented in 1977 by Prof. Iga [4]. A sketch of the actual design used in this publication can be seen in fig. 2.

The basic principle of the "gas sensing technique" is presented in Fig. 1. It bases on the fact that each gas in our atmosphere can absorb light. Depending on its special rotational, vibrational and electronic energy absorption spectrum different energies and to that effect wavelengths are needed for each gas type in order to be excited into the next higher energy level by laser light. The big challenge is now to design the emission wavelength of the laser accurately enough that it is close to the range of desired absorption line of the gas. By increasing the driving current of the VCSEL the emission wavelength also increases (this is called "thermally induced red-shift" of the device). This shift makes it possible to scan over a small wavelength range and as a result over the desired gas absorption line. By doing so the gas concentration of the investigated gas can be easily determined. This determination is accomplished by sending the laser light through the specific gas volume and by continuously measuring its intensity after having passed the gas volume. The measurement takes place during the whole tuning procedure of the laser wavelength. By the time the laser light is perfectly fitting to the gas absorption line the transmitted laser light intensity will dramatically decrease. This amount of intensity drop can be directly correlated to the gas concentration within the investigated gas volume. The big disadvantage of this tuning technique which is called "gain tuning" (change of the refractive index of the active region by increasing the driving current and heating it up) is the strongly limited tuning range. Only 4 to 7 nm tuning are available by this method for a VCSEL device lasing at 1.55 µm as central wavelength. This requires a very accurate and exact design and growth of the laser cavity for hitting the desired absorption line.

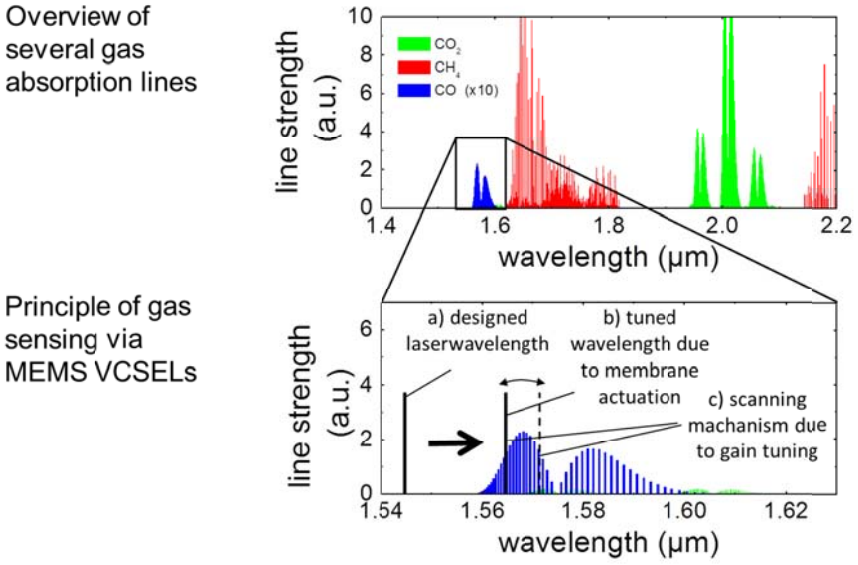

Fig. 1: Explanation of principles of gas sensing. *Top figure:* Gas absorption lines of H_2O, CO_2, CH_4 etc. over a wide spectral range being accessible by VCSEL structures. *Bottom figure:* Wavelength scanning technique of a VCSEL in order to reach the desired absorption line of the gas by a combination of comb mode and gain tuning mechanisms.

By contrast the so called MEMS VCSELs (Micro-Electro-Mechanical-System VCSELs) offer a much bigger tuning range. Their tuning concept is based on the "cavity-tuning" mechanisms. In this concept the geometrical length of the laser cavity is periodically varied which is also causing a change of the spectral position of the fabry perot modes of the laser resonator. And also in this case a shift of the emission wavelength towards higher wavelengths occurs. The simplest way of influencing the cavity length is to replace one of the laser mirrors by a movable membrane which can be electrically heated up and cooled down resulting in a periodic extension and shrinkage of the cavity length (details can be

found in chapter 3). The first concepts of MEMS VCSELs based on InP have been investigated and presented in [5]. As the tuning ranges of these VCSEL devices are nowadays exceeding even the 40 nm range the lasers and their emission wavelengths can be designed with much more tolerances [6]. This tuning principle of adjusting the laser wavelength of a MEMS VCSEL for reaching a special desired gas absorption line is demonstrated in fig. 1.

In general the MEMS VCSEL can be designed at a certain wavelength (see black left line (a) in fig. 1). It can be easily seen that the there is a huge distance in between the laser emission line and the really focused position of the gas absorption line (see blue comb spectrum). This spectral distance can be overcome by thermally actuating the membrane of the VCSEL that is by tuning the cavity length of the laser. As a result the original laser emission line is shifted into the red to the second displayed position (see fig. 1 black line (b)). From this point the gain tuning mechanism already discussed before is applied by periodically increasing and decreasing the driving current of the laser resulting in a small wavelength shift of the emission line scanning over the absorption line of the gas (see fig. 1: The dashed line represents the endpoint of gain related tuning range (c)). At this tuning mechanism the membrane is used to correct the spectral position of the laser emission whereas the real scan over the absorption line is accomplished by gain tuning. It should be noticed that in general the gain tuning is not necessary for the wavelength scan. The scanning procedure can also be solely realized by membrane actuations.

Hereby, the driving current through the VCSEL device will be kept constant whereas the MEMS VCSEL emission wavelength is designed in the range of some absorption lines of gases. A periodical heating up and cooling down of the membrane results in a periodic wavelength shift and scan over the fully available tuning range of the MEMS VCSEL. The tuning range of our nowadays manufactured MEMS VCSELs is already exceeding the 40 nm barrier. However one should take into account that this scanning mechanism is much slower than the one related to gain tuning.

These two ways of gas sensing form the basis of the so called TDLAS technique (Tunable Diode Laser Absorption Spectroscopy) being already implemented in many sensing products by well-known companies just like “Siemens AG” in Germany for example [7]. On the basis of these application fields VCSELs and in particular MEMS VCSELs have gained more attraction over the last years and had been found interesting and promising enough for justifying more detailed investigations on this topic in many institutes worldwide.

These ongoing investigations continuously improved the original VCSEL design and opened up many new ways of modifying the invention of the first fixed wavelength VCSEL designed in 1977 by Prof. Iga [4]. Devices had been developed showing on the one hand the inherent VCSEL specific longitudinal singlemode behavior combined with their compact design and their ability for on-wafer testing while on the other hand offering direct access to market oriented features like wide tunability, high-power or fast modulation properties. As the VCSEL properties and its wide field of applications became more and more perspective, big efforts had been done to extend the wavelength range to the 0.8 – 2.6 µm field. Therefore, a change of the substrates from GaAs to InP and finally to GaSb had been necessary. This transfer offered on the one hand very promising results as the far mid-infrared region had become instantaneously accessible, on the other hand showed some severe consequences resulting in a complete new reinvention of the whole VCSEL process technology as the already successfully established one on GaAs could not have simply been transferred to the InP or GaSb system. Besides the control of the process technology the epitaxy of the devices, which means the growth of the crystals, had been the other big challenge. Predominately the proper choice of lattice-matched Distributed Bragg Reflector (DBR) materials as mirror materials for the laser located on the top and the bottom side of the structure (see fig. 2) decided in many cases whether a specific VCSEL device could have been successfully realized or not. These DBRs must support the device with reflectivity values beyond 99% for assuring the desired round-trip of photons within every laser device in general.

As this reflectivity is again correlated with the different refractive indices of these DBR layers (Basic rule: The higher the refractive index contrast of the applied layers the less pairs of DBR materials are needed for exceeding the 99% reflectivity), one can imagine that these mirrors show a very big thickness due to the small index contrast of semiconductor based DBRs being located in the range of $\Delta n = n_2 - n_1 = 0.1$ to 0.3.

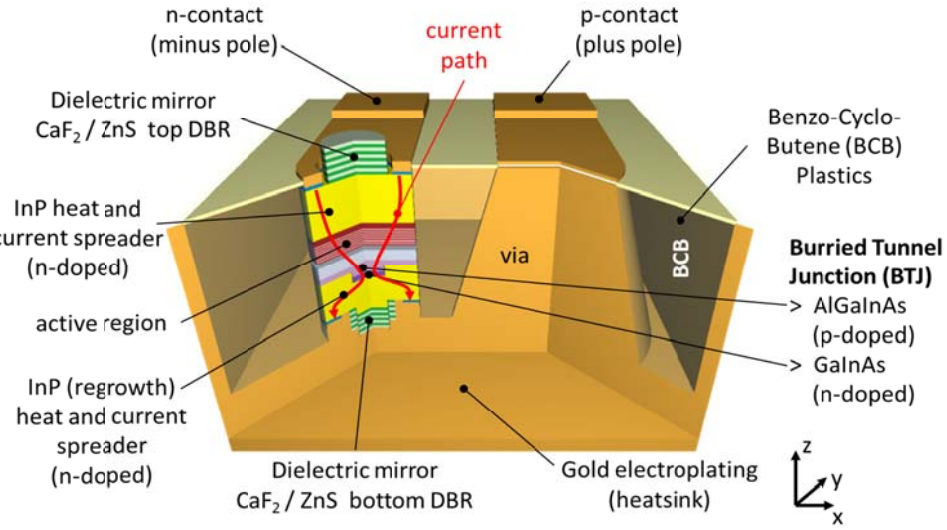

Fig. 2: Schematic cross-section of a InP-based BTJ (Burried-Tunnel-Junction) VCSEL. The device is mounted epi-down on a electroplated gold pseudo-substrate (see "integrated gold heatsink"). The InP substrate on the top is removed while manufacturing. Both n- and p-contact can be accessed there. Contact-pad capacitances are minimized by implementing BCB technology.

This leads to a remarkable increase of the longitudinal extension (see z-direction in fig. 2) of the VCSEL cavities up to the range of 8 µm for 1.55 µm devices and even more. As a result the electrical and thermal properties and in particular the heat management of the devices became gradually more important and are still under investigation nowadays. An overview over the present status concerning long-wavelength BTJ-VCSELs emitting at 1.3 – 1.55 µm allowing long-distance data transfer and optical spectroscopy can be found in [8-11].

Over the few past years it pointed out that InP based VCSELs can be considered as key optical sources in optical communications and gas sensing showing simpler fiber coupling, wide tunability, easier packing and testing as well as the ability to be fabricated then in arrays. Additionally, their cost-effectiveness and low power consumption supported their rapid commercialization in metropolitan areas and wide area network applications and sensing products being used for **T**unable **D**iode **L**aser **A**bsorption **S**pectroscopy (TDLAS).

2. DEVICE STRUCTURE

The structure shown in fig. 2 is the actual investigated design in this paper. On the basis of this structure all the following measurements had been carried out. The primary aim when having designed this new structure had been to develop a VCSEL which shows much better thermal properties compared with all the previous devices. The heat management can be considered as one of the basic aspects determining whether a device works or not. Additionally a very efficient way of subtracting the heat out of the device serves very profitable for every single and further going device property itself. In the following subsections we are describing in detail which components had been changed in what way in order to fulfill expectations we had in mind with respect to high-speed and wide tunability.

2.1 Top and bottom mirrors (Distributed Bragg Reflectors – DBRs)

By contrast to the former VCSEL structures this modified VCSEL does not have an epitaxial mirror on the top (see fig. 2). It has been replaced by a 5 paired dielectric one. The same has been accomplished for the bottom DBR. Here only 3.5 pairs are implemented due to the gold electro plating at the bottom of the device. Typical dielectric materials are AlF_3 and ZnS. The big advantage of these materials is their bigger refractive index contrast with respect to the InP related lattice matched semiconductor materials. While InP lattice matched AlGaInAs and AlInAs semiconductor based DBR layers show refractive index contrasts of about $\Delta n = 0.3$ the dielectric materials have a much larger value of

approximately $\Delta n = 1.0$. Consequently one would need more than 30 pairs of AlGaInAs/AlInAs-pairs in order to reach the desired reflectivity of beyond 99% but only 5 pairs of AlF_3/ZnS. As every DBR layer independent of dielectric or semiconductor based must have an optical length of a quarter of the cavity wavelength (in our case 1.55 µm) the thickness of the whole semiconductor DBR reaches values of approximately 7 µm (30 x 112 nm for AlGaInAs plus 30 x 121 nm for AlInAs, respectively). One can imagine that this DBR thickness is undoubtedly raising both the electrical and the thermal resistance of the device as the current has to flow through the whole top DBR before reaching the active region (this old concept has been presented in [5]). By contrast the 5 paired AlF_3/ZnS DBR shows a thickness in the range of 2.2 to 2.6 µm.

We have got rid of this disadvantage by simply implementing the AlF_3/ZnS dielectric DBR and making a short-cavity device out of the former VCSEL design with intracavity current injection. Intracavity current injection means that the current does not have to pass all DBR layers before reaching the active region. The contact ring (see "n-side contact" in fig. 2) is surrounding the top DBR. Consequently as the current has to flow from this n-contact ring right via the InP "n-cladding" to the middle of the device, that is to the buried tunnel junction situated in the center, the electrical resistance is now predominantly determined by the radius of the n-side contact ring. This resistance is called the "spreading resistance" and can be easily calculated by the formula $R = \rho \cdot l/A$ where ρ is the specific resistance of the bulk InP n-doped material, l is the radial distance of the contact ring from the central axis of the device and A is describing the cylindrical sidewall through which the current passes when being injected at the ring contacts. A simple integration over cylindrical side walls leads to the resistance R. Beyond these basic dependencies for the laterally determined electrical resistances the thickness of the InP heat and current spreader (see fig. 2) is another very important parameter. Some qualitatively held discussions on this topic will be given in the next chapter 2.2.

2.2 The InP current and heat spreader

Our present VCSEL device mainly consists of thick InP layers on both sides (see "InP n-cladding" and "InP regrowth" in fig. 2). As the current has to pass through these layers (see red curve in fig. 2) their thicknesses directly control both the electrical and thermal resistance of the device. We have done simulations on the basis of "COMSOL Multiphysics ®" and have experienced that this thickness is even the most influencing part of the device considering the thermal properties. Some basic rule of thumb would be: The thicker these two spreading layers the more efficient is the heat transfer. So for high-speed and high-power devices a very thick InP heat and current spreader on the bottom and on the top of the whole structure would be very promising. However the longer the cavity length in *z*-direction (see fig. 2) the smaller the so called free spectral range (FSR) and the smaller is the tuning range of the device. Considering our intention to build a device suitable for gas sensing, spectroscopy and perhaps being suitable for integration in fibre bragg gratings this restriction in tuning range would be a tremendous disadvantage although the heat management might be properly set. As a result we have chosen a thickness of around 1.1 µm for both sides (bottom and top InP layer) in order to take this trade-off into account.

The red line in fig. 2 indicates now the current path by the time some bias is put on the device contacts. Right in between of the both already discussed InP heat and current spreading layers the buried tunnel junction is situated. The buried tunnel junction serves as can be seen as a sort of current confinement and optical aperture defining the beam waist within the cavity.

2.3 The Burried Tunnel Junction (BTJ)

As the current is injected in a circular geometry with a remarkable distance from the middle axis of the device one needs some aperture or confinement layer which confines the current at the center in order to guarantee a sufficiently high current density in the active region. This is accomplished by the so called buried tunnel junction (BTJ), see fig. 3 [12,13, 14]. The BTJ is consisting of two very highly doped layers, namely AlGaInAs (highly p-doped, $p = 1.5 \times 10^{20} cm^{-3}$) and GaInAs (highly n-doped $n = 1.5 \times 10^{20} cm^{-3}$). Due to the high doping the bandedges are getting deformed by the time the device is biased. The band edge deformation can be seen in fig. 3.

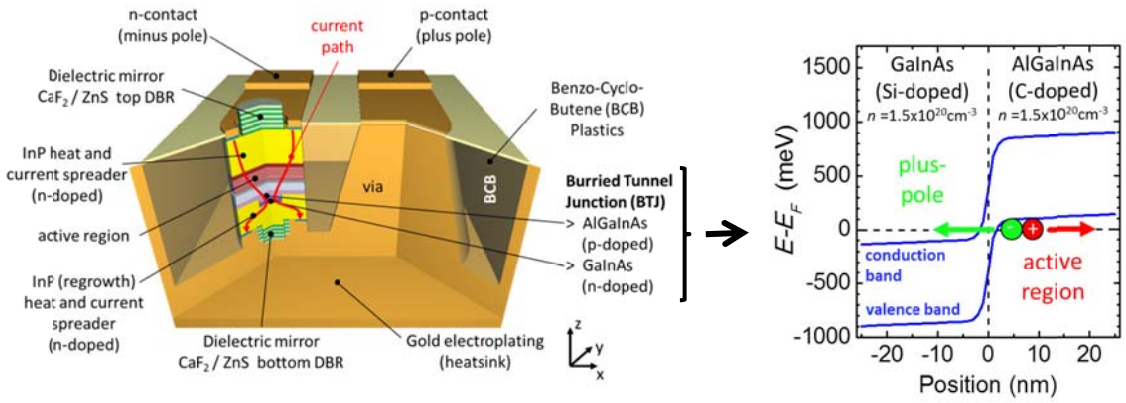

Fig. 3: Shape of the band edges of the conduction band and the valence band of a standard BTJ (p^{+-}-AlGaInAs versus n^{+-}-GaInAs). The BTJ is lattice matched to InP. The dashed line shows the Fermi level and the position at which a carrier conversion occurs.

2.4 The active region

The origin and the place where most of the discussed heat is generated is right the middle of the active region. In this part of the VCSEL the carriers (electrons coming from the n-pole and holes coming from the p-pole of the device) are recombining and light is generated. The heat which is getting evolved over there will then be transferred to the surrounding layers on the top and on the bottom of the device and especially by the gold electroplating on the bottom. The active region itself consists of highly compressively strained AlGaInAs quantum wells (QWs) with a thickness of 6 nm. These wells are separated from each other by 7 nm thick lattice matched AlGaInAs barriers (the QW material shows of course another material concentration then the barrier one although they are carrying the same name). "Compressively strained" refers to the fact that the lattice constant of these layers is slightly different to the one of the InP substrate. As a result these layers experience a lateral force being originated by the InP substrate. By the time the lattice constant of the grown layer is bigger then the InP one compressive strain within the plain direction is occurring. This compressive strain is a very useful tool in order to dramatically increase the differential gain of the active region [15]. As we are planning to realize a widely tunable device being also suitable for high-speed data transmission (that is telecommunication) the active region should not only deliver the necessary broad gain for wide tunability but also a good value of differential gain and of f_{3dB} frequency being a direct measure for the high-speed characteristic of a VCSEL device. The present world record value is at present given by our InP based short cavity (SC) VCSEL devices with 17 GHz [16]. A slightly further improvement of these devices could make them suitable for the nowadays asked 100G-LR4 standard (4 x 25 Gbit/sec data transmission), the high-speed devices of the future being the basis of 3 dimensional television, USB 3.0, ultra-high definition TV, telepresence etc.. Next to this modification of the active region there are several discussions about how to artificially increase the full width at half maximum (FWHM) of the gain curve of the active region for getting wider tuning ranges. However this is a very actual topic of investigation today.

Another very important design aspect of the active region is the so called mode gain offset. It is not said for sure that the active region is also designed for 1.55 µm if the cavity or resonator is done so. One has to take into account that the gain curve is also shifting by increasing the temperature of the device. The higher the temperature the bigger the emission wavelength being considered as a redshift of the central wavelength. One very important tool for a thermal improve of the device is the proper adjustment of the central wavelength of the active region with respect to the design of the cavity. This is the so called "mode-gain offset". Our newly designed device for instance has a mode-gain offset of 45 nm. The cavity is designed for 1.555 µm whereas the emission of the quantum wells is situated at around 1.510 µm. By the time the device is lasing at room temperature (25°C) the gain curve is not perfectly fitting to the resonator design. However when heating it up to temperatures beyond 60°C the gain peak shifts more and more to higher wavelengths and starts to fit better and better to the whole cavity design (see fig. 7b for shift of emission wavelength due to temperature increase). This leads to the fact that the device is perfectly working at higher temperatures beyond 60°C and not only at 20°C and lower.

2.5 The standing optical wave within the resonator – modulation doping

By the time the laser is working the photons inside the cavity are building up a so called optical standing wave, defining the wavelength which is able to propagate within the cavity structure. The calculation of these optical standing waves can be done by the transfer matrix method [17]. This method is very well known in optics. Electromagnetic waves propagating through lenses and dielectric media can be easily described by this method as each lens will be mathematically replaced by a matrix showing certain diffraction, transmission, loss properties etc. When using this mathematical technique for describing the propagation of photons within our VCSEL cavity then the following optical standing field occurs (see fig. 4). The black lines within the window represent the refractive index of the different VCSEL layers. The left end of the window shows a rectangular structure representing the top DBR consisting of 5 pairs of AlF_3/ZnS, whereas the right side represents the bottom DBR (3.5 pairs of AlF_3/ZnS). The bulk structure in the middle with a small peak represents the refractive indices of both InP heat and current spreaders sandwiching the active region and the BTJ in the middle (see the narrow spike in the middle of the picture in fig. 4). The red curve is the above mentioned standing optical field pattern within the VCSEL cavity. As one can see minima and maxima are occurring when following the red line from the left end of the structure to the right end. It is pretty obvious that at those places where a maximum of the standing wave occurs the doping of the semiconductor layers should not be too high. Otherwise the VCSEL suffers from high optical absorption losses while lasing. The optical output power would then be dramatically decreased and the whole device would not be suitable for any kind of application at all, neither high-speed, high-power nor wide tunability.

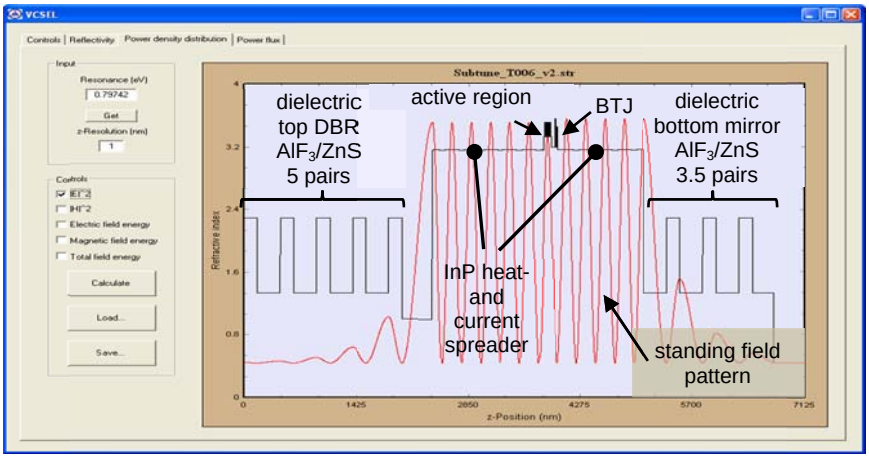

Fig. 4: Simulation of the optical standing field within the VCSEL cavity by the simulation program called "VCSEL" from the company VERTILAS GmbH [18]. The program is based on transfer matrix calculation methods for evaluating the field pattern.

The adaption of the doping sequence within the VCSEL structure is called "modulation doping" [17] and has also been optimized in the present new structure in a way that the layers are doped highly enough ($2x10^{18}cm^{-3}$) for assuring a good electrical resistance on the one hand, on the other hand implement enough lowly doped layers ($5x10e^{17}cm^{-3}$) for keeping the optical absorption losses at a minimum value.

3. PRINCIPLES OF TUNING AND WIDE TUNABILITY

In chapter 2 we have discussed all relevant components of the present VCSEL. On this basis we can now go further into detail for getting an idea how the tuning mechanism can be accomplished in VCSEL devices (see also [19]). In chapter 4 our present results on the basis of this design will be discussed.

3.1 Basic laser components and free spectral range

As any other laser also the VCSEL consists of the three basic components (see fig. 5a):

a) Two mirrors (mirror 1 and mirror 2) which are forming the Fabry-Perot resonator. The resonator defines the modes which are able to build up standing waves within the cavity (see upper right picture in fig. 5a). It is important to mention that these modes show a very strict spectral distance among each other, the so called free spectral range (FSR) which is defined as [19]

$$FSR = \frac{\lambda^2}{2nL_{cav}}$$

The spectral spacing is consequently indirect proportional to the optical cavity length nL_{cav}. This FSR is besides the spectral broadness of the gain curve the second very important parameter defining the width of the tuning range of the VCSEL device. The smaller the cavity extension in z-direction the larger the tuning range. That is why a larger InP heat and current spreading layer (see fig. 2) might be profitable for the heat management of the device but not for the width of the tuning range (see also subsection 2.2).

b) The active region has already been discussed in chapter 3: It supports the whole device with a certain gain curve determining the modes which are experiencing enough gain in order to exceed the total losses of the device and can potentially start lasing. The sketch in the middle right of fig. 5a is very important to understand afterwards, in combination with fig. 5b, the special behavior of wavelength change dependent on the airgap size by the time the cavity is extended.

c) The pumping of the VCSELs can be accomplished electrically or optically. The device above is pumped electrically. The electrical pumping is also responsible for the fact that the spectral maximum position of the gain curve shifts to higher wavelengths by the time the device is pumped harder (gain-tuning) as already mentioned in the introduction of this publication.

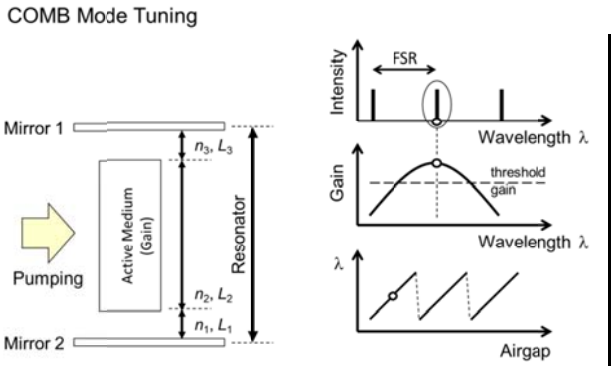

Fig. 5a: Laser in the fixed wavelength case. No comb mode tuning has occurred. The laser wavelength is exactly situated in the center of the whole tuning range.

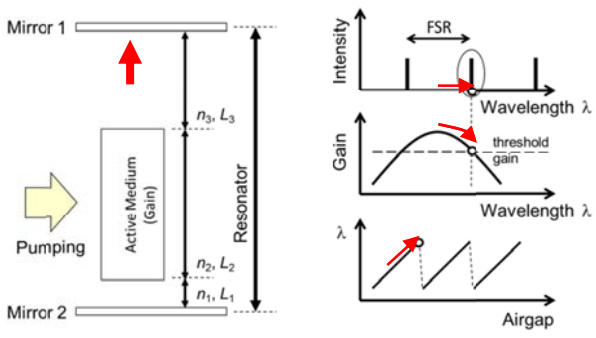

Fig. 5b: Laser is fully tuned to the end of the tuning range. A further increase of the cavity length with force the laser to start at the beginning of the tuning range again.

The word MEMS meaning Micro-Electro-Mechanical-System offers direct access to wide tunability. Fig. 5b shows what happens by the time mirror 2 is thought to be fixed and mirror 1 is movable. When extending the cavity length of the resonator by moving mirror 1 further in the upper direction, the displayed three modes in the upper right sketch of figure 5a start moving to the right in direction to higher wavelengths. When having a look at fig. 5b at the middle right sketch it is striking that the dot is situated at the very etch of the gain curve at which the gain equals the internal losses of the device. By the time the cavity is further extended, this point (representing the emission wavelength of the laser device) will move further on along the gain curve right below the "threshold gain" line and will not any longer have the

possibility to lase as the gain curve is below the horizontal line of internal losses. However, at the left side of the gain curve of fig. 5b middle right the next Fabry Perot mode is entering the high-gain regime where enough gain is available to compensate all internal cavity losses. At this point the laser again starts lasing at the very beginning of the tuning range. This behavior keeps going on and on by the time the cavity would be extended further and further. At the bottom right of fig. 5a and fig. 5b one can see the outcome of this tuning procedure. The available wavelengths show a sort of "saw shape" structure when being plotted over the airgap extension whereas every single "tooth of the saw" represents the tuning range of every single Fabry Perot mode being shiftet through the whole continuous tuning range.

According to our VCSEL structure this principle of a moving mirror can be realized by simply cutting off the upper DBR from the VCSEL device and generating a half VCSEL structure plus an external membrane which can be thermally actuated by current injection (see fig. 6). By thermally actuating the membrane the cavity length of the device can be changed and the wavelength will be tuned. The former tuning ranges of the previous VCSEL devices had been in the range of 54 nm [5]. These devices have been single mode with side mode suppression ratios around 50 dB and output powers in the milli-Watt regime. However, the high-speed property of those devices had not been in a competing range worldwide. Fig. 6 also shows a microscope picture of the membrane under which one can clearly see the airgap. As a conclusion up to know we can state that we can build VCSEL devices with a fixed top DBR being suitable for high-speed and high-power applications and on the other hand VCSEL devices with an external top mirror in form of a membrane being mainly suitable for wide tunability. On the basis of these theoretical and partially experimental results our newly developed device will be tested now and the present high-speed, high-power and tunability properties will be presented.

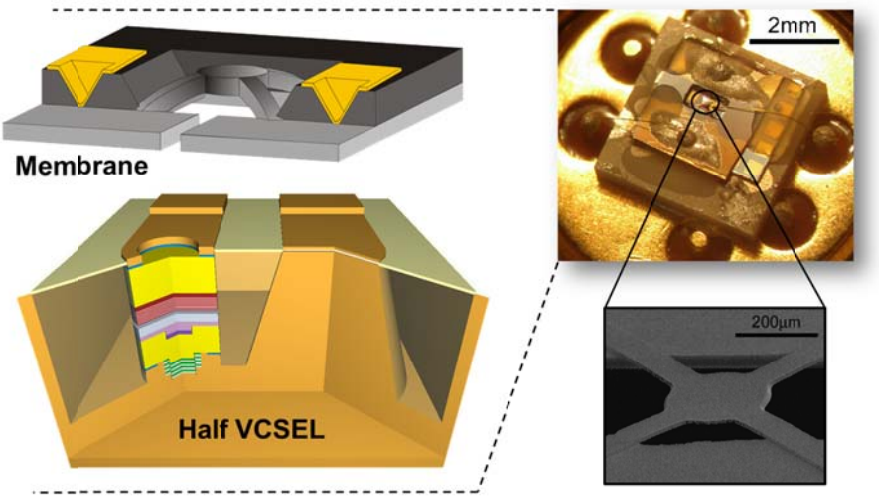

Fig. 6: Realization of the MEMS VCSEL concept with a movable top mirror membrane which can be thermally actuated. Its deflection is directly correlated to the emission wavelength of the VCSEL device.

4. THE PRESENT VCSEL RESULTS

4.1 General Information

When we have designed the VCSEL structure shown in fig. 2 we thought about a basis structure being theoretically suitable for all three already numerously mentioned fields of application namely high-speed, high-power and wide tunability. Of course, all three properties cannot be achieved by one single device. But one single basis structure can theoretically have the possibility to satisfy all three goals depending on how this basis structure is finalized. With the word "finalizing" we are meaning the last step when evaporating the top DBR on the processed VCSEL structure. In

general two different ways of finalization exist whereas each of them forces different and completely not combinable device properties.

a) *Evaporation of a top DBR on the half-VCSEL structure*
This device for instance with evaporated AlF_3/ZnS DBR layers is shown in fig. 2 and is called "short cavity SC-VCSEL device". The reason for this expression is that on the basis of this technique the cavity length can be dramatically reduced which is heavily increasing the f_{3dB} frequency of the device ending up in very good high-speed properties predominantly suitable for telecommunication applications.

b) *Mounting of a semiconductor or dielectric based membrane on top of the VCSEL structure*
When gluing a membrane structure on top of the processed VCSEL the device is called MEMS VCSEL. Due to the thermally based actuation of the membrane the cavity length of the whole device can be easily modified resulting in a large wavelength shift beyond 40 nm. When thinking of gas sensing applications this technique is the most outstanding and promising one as it offers devices with flexibly adjusting emission wavelengths matching perfectly to the investigated gas absorption line in the spectrum (see description in the introduction and [20,21]).

The technique mentioned in a) is a very useful and relatively quick methode to check whether the processed VCSEL basis structure works or not determined via electro-optical and thermal characterization methods. This information will be kept in mind when afterwards finalizing another half-VCSEL structure with a top membrane in order to gain direct access to the field of gas sensing.

4.2 Device results

When finalizing the VCSEL basis structure by the technique a), the above mentioned high-speed short-cavity devices are generated. As no airgap is occurring with respect to this process step the device is representing a fixed wavelength device where only the internal heating of the active region by increased electrical pumping can cause a wavelength shift due to the above mentioned red shift of the gain curve. This so called "gain tuning" is in the range of 4 to 7 nm. In fig. 7 the first results of these devices are shown. This figure is divided into three parts whereas the left part (fig. 7a) shows the high-speed measurements, the middle part (fig. 7b) shows the *L-I-V* properties (light-current-voltage) and fig . 7c on the right takes into account the suitability of the device for gas sensing applications that is tunability.

Considering the electrical properties of the devices (see fig. 7b) the voltage drop over the fully applied current range from 0 to 27 mA shows reasonable values with a kink voltage of approximately 0.9 V and a maximum value of 2.1 V. This current-voltage curve does not vary over the full considered temperature range from 20 to 80°C. The optical output power of the devices shows maximum values of 6.7 mW at room temperature and even 3 mW at 80 °C. There has never been published values like this for an InP based VCSEL with a BTJ of 5.5 µm. These very high output powers are indeed a confirmation of the above mentioned heat reducing components which had been implemented in the present VCSEL structure. The lower part of fig. 7b additionally shows that also the single mode property of the device is not suffering from increasing the peltier element temperature from 20 to 80°C. The SMSR shows values of at least 50 dB over the whole temperature range proving the highly single mode property of the device. In general a device can be claimed as "single mode" by the time the neighboring peak within the emission spectra shows an intensity which is 30dB smaller with respect to the main peak.

As this device has been mainly designed and optimized for high-power and good thermal heat management one would already expect that the high-speed properties of these devices are not beating the present world record values. Nevertheless their values are undoubtedly in a very useful und applicable range. In fig. 7a the high-speed measurements of the devices are shown both at room temperature and 80°C. It can be stated that the f_{3dB} value representing the high-speed property of a device is always beyond 11 GHz even at 80°C. This means that these devices can be applied for data transmission in the 12.5 Gbit/s range for each desired and specified temperature within 20 and 80°C. The best state of the art high-speed short cavity VCSELs realized within our group are reaching the present world record values of f_{3dB} of 17 GHz (see fig. 7a bottom). More detailed information about high-speed short-cavity VCSELs can be found elsewhere [9-11] and will not be discussed here as gas sensing applications are not requiring high-speed properties.

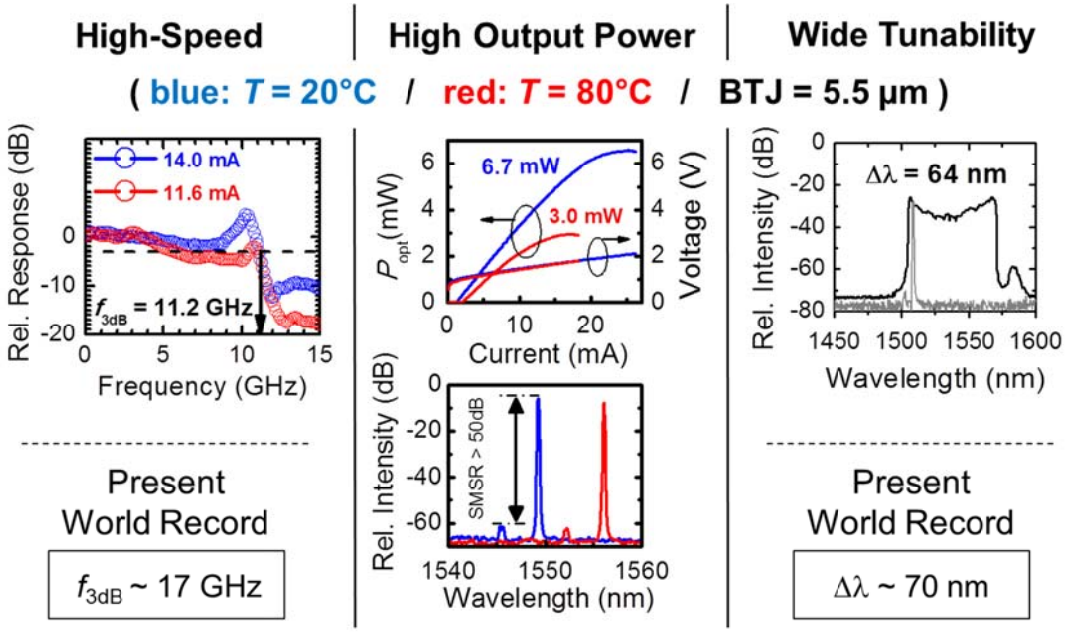

Fig. 7a: *Top:* High-Speed measurements of the realized fixed wavelength VCSEL. It is striking that the f_{3dB} frequency seems to be stable over 11 GHz over the whole temperature. *Bottom:* Present world record value of f_{3dB} realized by Technical University of Munich – Walter Schottky Institute [16].

Fig. 7b: *Top:* LIV-curves (light-current-voltage) of the realized fixed wavelength VCSEL. *Bottom:* Emission spectra of the fixed wavelength short cavity VCSELs finalized via methode a) showing a SMSR exceeding 50dB over the whole temperature range. These values represent world record ones.

Fig. 7c: *Top:* Tuning range of the VCSEL achieved with external flat dielectric piece of DBR wafer put on top of the laser. *Bottom:* Present world record of tunability achieved by Technical University Darmstadt (half-VCSEL structure realized by Technical University Munich – WSI) [22].

To examine the laser with respect to wavelength tunability, also some preliminary tests with a bulk flat DBR have been accomplished. The measurement principle is presented in Fig. 8. The plane piece of DBR is put on top of the laser and fixed with two needles. One can easily change the tilt of the top mirrors by alternating the force on the plane being exerted by the needles. This easy method allowed us to quickly test the laser tuning capability and demonstrates a laser wavelength tuning of more than 60 nm (Fig. 7c).

The bulk mirror consists of 11 pairs of Si_3N_4 / SiO_2 deposited by ICP-CVD (Inductive Coupled Plasma-Chemical Vapour Deposition) [23] on a 350 µm thick GaAs substrate. Each layer has an optical thickness of λ/4. The λ/2 Si_3N_4 layer in-between serves as adhesive layer. For the suppressing the reflectivity of the GaAs, a λ/4-layer anti-reflection coating (ArC) of SiO_xN_y is deposited onto the bottom side. Because of the high refractive index contrast of 0.55 between the dielectric layers, the wide stop bandwidth higher than 200 nm and required reflectivity of more than 99% can be reached.

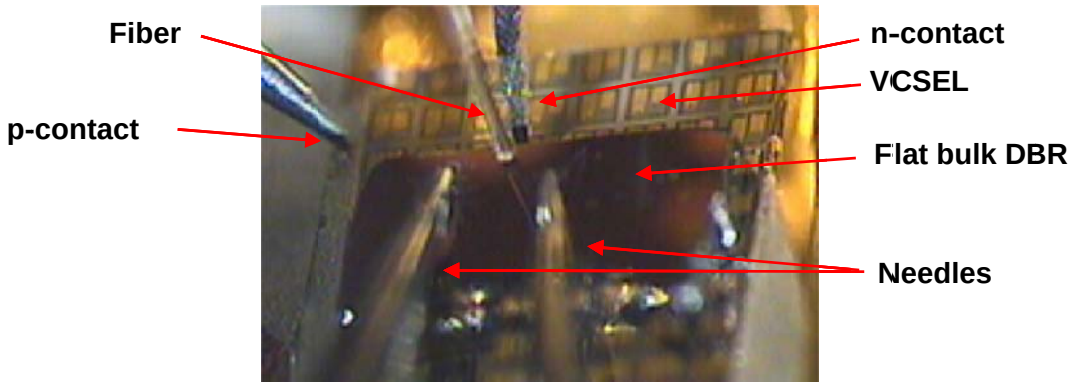

Fig. 8: The tuning of the laser wavelength by the use of a plane bulk dielectric DBR.

5. CONLUSION

We have realized half-VCSEL structures being perfectly suitable for both high-speed and wide tunability that is telecommunication and gas sensing. The realized fixed wavelength VCSELs with a 5 pair AlF_3/ZnS top DBR show world record optical output powers of 6.7 mW at room temperature and 3 mW at 80°C. The voltage drop is within a range from 0.9 to 2.1 V. Due to the perfect heat management of the device we have also observed single mode behavior for 5.5 µm BTJ diameters over the whole temperature range with side mode suppression ratios (SMSR) exceeding 50 dB. Concerning gas sensing applications preliminary tests of tuning capability using a bulk flat dielectric DBR have shown a cavity tuning over 60 nm. In the next steps we will investigate the mounting of an electro-thermally actuated MEMS-DBR with concave mirror membrane as described in section 3. Although the device has been predominantly designed and optimized for an efficient heat subtraction, the high-speed properties are also very promising showing stable f_{3dB} values of 11.2 GHz over the whole temperature range being perfectly suitable for 12.5 Gbit/s data transmission applications. In the following the high-speed properties of the two-chip MEMS VCSELs and also measurements about SMSRs and thermal resistances will be done. Besides we are planning to produce monolithically integrated MEMS VCSELs being more suitable for mass production as manufacturing costs dramatically decrease when overcoming this two-chip concept by a monolithic one.

REFERENCES

[1] Homepage of SUBTUNE-project, EU-project nr. 244259 (http://www.subtune.eu)
[2] G. Totschnig et al., Appl. Phys. B **76** (2003) 603.
[3] M. Lackner et al., Meas. Sci. and Technol. **14** (2003) 472.
[4] K. Iga, Invited Review Paper, Japanese Journal of Applied Physics, Vol. 47, Nr. 1, pp. 1-10, 2008
[5] Dissertation, Markus Maute, Walter Schottky Institut, Technische Universität München, "Mikromechanisch abstimmbare Laser-Dioden mit Vertikalresonator", Vol.81, ISBN 3-932749-81-2
[6] B.Koegel et al., ECOC, vol.2, Paper Tu3.4.4, pp.81-82, Cannes, France, Sept. 2006.
[7] J. Chen et al., CTuA4, CLEO 2009
[8] M.C. Amann et al., IEEE JSTQE, 15, 861-868 (2009)
[9] A. Syrbu et al., OFC/NFOEC, San Diego, CA, OThS2, 1-3, 2008
[10] M. Müller et al., CLEO 2010, San Jose, CA paper CME5, 2010
[11] M. Müller et al., IEEE PTL, 21, 1615-1617, 2009
[12] M. Ortsiefer et al. Jpn. J. Appl. Phys., Vol. 39, pp. 1727-1729, Part 1, No. 4A, April 2000
[13] M. Arzberger et al., Electronics Letters, Vol. 36, No.1, Online No. 20000039, January 2000
[14] Manish Meta et al., IEEE Journal of Quantum Electronics, Vol. 42, No. 7, July 2006
[15] S. Healy et al., IEEE J. Quantum Electronics, Vol. 46, No. 4, pp. 506–512, April 2010.
[16] M. Müller et al., International Semiconductor Laser Conference (ISLC), September 26-30, Kyoto 2010

[17] Dissertation, Markus Ortsiefer, Walter Schottky Institut, Technische Universität München, "Langwellige Vertikalresonator-Laserdioden im Materialsystem InGaAlAs/InP", Vol. 35, ISBN 3-932749-35-9
[18] Homepage of the company VERTILAS (www.vertilas.com)
[19] "Tunable Laser Diodes and Related Optical Sources", J. Buus, M. C. Amann, D. J. Blumenthal, Wiley-Interscience, ISBN 0-471-20816-7
[20] B.Koegel et al., ISOT, SPIE 7266B, Paper 5.4, San Diego (CA), USA, Nov. 2008.
[21] S. Schilt et al., Applied Physics B (2010) 100: 321-329, August 02, 2010.
[22] S. Jatta et al., Photonics Technology Letters, IEEE, vol.21, Issue: 24, San Diego (CA), USA. Dec. 2009
[23] S. Jatta et al., Plasma Processes and Polymers, 6, pp. 582-587, 2009

ACKNOWLEDGEMENTS

We wish to acknowledge the support of the European Commission on the basis of the EU project SUBTUNE, EU-project nr. 224259 within the seventh framework program.